www.czasopisma.pan.pl PAN POLSKA AKADEMIA NAUK www.journals.pan.pl

Arch. Metall. Mater. **62** (2017), 1, 405-410

DOI: 10.1515/amm-2017-0063

P. LEDWIG*#, M. KOT*, T. MOSKALEWICZ*, B. DUBIEL*

ELECTROPHORETIC DEPOSITION OF nc-TiO_2/CHITOSAN COMPOSITE COATINGS ON X2CrNiMo17-12-2 STAINLESS STEEL

This paper presents the results of the optimization of electrophoretic deposition parameters for manufacturing of nc-TiO_2/chitosan composite coatings on X2CrNiMo17-12-2 steel as well as characterization of their microstructure, electrochemical properties and adhesion to the substrate. The parameters of the deposition, such as composition, pH and zeta potential of suspensions as well as voltage and process time were investigated. The microstructure of the coatings was characterized using scanning and transmission electron microscopy. Obtained coatings were crack-free and uniform. The adhesion strength to the substrate was measured by scratch-test method. The deposited coatings improve corrosion resistance of steel, what was confirmed by the results of the potentiodynamic polarization test in Ringer's solution.

Keywords: chitosan; TiO_2; electrophoretic deposition; X2CrNiMo17-12-2 steel

1. Introduction

Stainless steel is commonly used in biomedical applications. This material is characterized by good mechanical properties and it is cheaper than titanium and cobalt alloys [1,2]. Nevertheless, uncoated stainless steel exhibits not sufficient corrosion resistance in environments containing Cl^- ions, which are present in human body fluids [3,4]. For this reason it is widely used as short-term orthopedic implants. In order to improve the corrosion resistance, the steel can be modified or coated by other material, which exhibits better corrosion properties [5]. One of materials groups characterized by a good corrosion resistance are oxides, for example SiO_2, TiO_2, Al_2O_3 and others [3]. For biomedical applications it is also essential to create a material which would be biocompatible. TiO_2, in addition to its good corrosion resistance, is biocompatible. It can appear in three mineral forms, namely rutile, anatase and brookite. Between them anatase exhibits antibacterial properties [6], which significantly accelerate the process of healing after implant's application [7-9]. Most of the sintered high density coatings have poorer biological properties than unsintered ones with high surface area [10]. Additionally, chitosan, which bounds the TiO_2 particles to the surface and improves its adhesion to the metal, can be used as component of corrosion resistant composite coatings [9]. Chitosan is a polysaccharide, produced by deacetylation of chitin, which has a proven biocompatibility and antibacterial properties [11].

TiO_2 deposition on metal surface can be executed by use of many techniques, such as plasma spray technique [12,13], sol – gel [14,15], micro arc oxidation [16,17] and electrophoretic deposition (EPD) [18-21]. Chitosan, as biopolymer, is destroyed by high temperature. Due to this fact its deposition can be performed only by use of low temperature techniques, like EPD. The EPD method belongs to the group of electrochemical deposition methods, which allow to obtain wide variety of homogenous, high-purity coatings [22]. It gives the possibility of application of different types of materials, and also deposition of composite coatings. In this technique the electromagnetic field is applied between two electrodes immersed in suspension. The particles are charged in the suspension and move to the electrode with the opposite charge, where they are deposited. In EPD method many organic and inorganic solvents can be used. In case of TiO_2 deposition from suspensions containing acetone or acetylacetone [23] may be used. It is also possible to use water and ethanol-water suspensions [18-20], what is very important for biomedical applications, because they are less toxic. In the case of deposition of chitosan the most commonly used solvents are water or water-ethanol mixture. Water ensures high electromobility of the particles and ethanol increases stability of the suspension [22]. The mechanism of EPD of chitosan in aqueous-ethanol media is well known and described elsewhere [24]. Based on Zhitomirsky and Hashambhoy results [24], in our work a water-ethanol system was selected to deposit nc-TiO_2/chitosan, because in acidic water-ethanol suspension amine group of chitosan receives a positive charge. Locally, near to cathode, the decomposition of water takes place thereupon on metal surface basic pH is being created. Chitosan becomes insoluble in basic pH and loses its positive charge what causes a creation of insoluble deposit on the surface.

* AGH UNIVERSITY OF SCIENCE AND TECHNOLOGY, 30 A. MICKIEWICZA AL., 30-059 KRAKÓW, POLAND

Corresponding author: pledwig@agh.edu.pl

The aim of this paper is the choice of optimised parameters of deposition composite coatings containing nanocrystalline TiO_2 and chitosan on X2CrNiMo17-12-2 steel, as well as characterization of their microstructure, electrochemical properties and adhesion strength to the substrate.

2. Materials and methods

For the preparation of the suspensions, TiO_2 nano-powder (21 nm particle size, Aldrich) and chitosan (deacetilation 75 – 85%, medium molecular weight, Aldrich) as well as distilled water and ethanol (99.8% pure, POCH) were used. The concentration of chitosan was equal to 0.5 g/L and concentration of TiO_2 varied between 0.5 and 3.0 g/L. The suspensions were prepared by stirring chitosan with solvent for 24 hours and subsequently for another 30 minutes with the TiO_2. Prior to the deposition, obtained suspensions were dispersed ultrasonically by 30 minutes. During the process of deposition suspensions were stirred to ensure the good dispersions of TiO_2. The zeta potential (ζ) and stability of suspensions were measured using ZetaSizer Nano-ZS 90. The suspensions' pH was gradually changed by addition of acetic acid (99.8% pure, POCH) and NaOH. Constant distance between electrodes was 10 mm. The deposition was carried out in the voltage range 5-50 V. The process was performed at room temperature, under atmospheric pressure. Both electrodes were made of X2CrNiMo17-12-2 austenitic stainless steel (known also as AISI 316L). Chemical composition of the steel is the following (in wt %): ≤0.03 C, 17.5 Cr, 11.5 Ni, ≤2.0 Mn, 2.3 Mo, ≤0.11 others, Fe balance. Before deposition, the electrodes (dimensions of plates: 29×15×0.5 mm) were polished on abrasive papers of 2000 gradation, cleaned in distilled water and ultrasonicated in ethanol for 15 minutes. After deposition the coatings were dried at room temperature during 24 hours.

Scanning electron microscopy (SEM) investigation was carried out for plan-view specimens of the coatings using Jeol NeoScope JCM-6000 microscope at the accelerating voltage 15 kV. Transmission electron microscopy (TEM) investigation was performed by means of Jeol JEM-2010 ARP microscope to examine the TiO_2 nanoparticles used in suspensions as well as the microstructure of the deposited coatings.

For TEM analysis of TiO_2 nanoparticles, their suspension in ethanol was dropped on the copper grids and dried. The thin lamella from the cross section of the nc-TiO_2/chitosan coating deposited on steel substrate was prepared using Focused Ion Beam (FIB) method using FEI QUANTA 3D 200i.

The surface roughness and coatings' thickness measurements were performed using the optical profilometer WYKO NT930. The observed representative areas were situated in a central part of the coating. The step between coatings and the uncovered substrate was formed by scratching. The thickness of the coating was calculated as the altitude of this step on the profile. Additionally, the thickness of the coating was measured on TEM images of the cross-section specimen.

The adhesion strength of the coatings to the substrate surface was measured in scratch-test by means of Micro-Combi-Tester, CSM Instruments. The length of the scratching track was 5 mm. The tests were carried out with a load 0.03-5 N and the constant speed of the intender 5 mm/min. Microstructural investigation of the scratch tracks was performed by means of light microscopy (LM).

The electrochemical properties of the coatings were determined by the potentiodynamic polarization test in Ringer's solution. The curves were acquired using a potentiostat/galvanostat Autolab PGSTAT 302N. The measurement was performed in three-electrode system, where platinum wire was a counter electrode and reference electrode was Ag/AgCl. Tested was area of 1 cm^2 was limited with lacquer.

3. Results and discussion

To provide both a good stability and a high electrophoretic mobility of the TiO_2 nanoparticles, the suspensions used for electrophoretic deposition of TiO_2/chitosan coatings were based on the mixture of distilled water and ethanol. The mixture used for deposition of composite coating contained 50% ethanol, 49% water and 1% acetic acid (vol. %). This composition of liquids provided good stability and good dynamism of deposition.

To determine the stability of the TiO_2, chitosan and TiO_2/chitosan suspensions, the measurements of zeta potential in the function of pH were performed. The pH was adjusted by addition of CH_3COOH or NaOH. The measurements were carried out with concentration reduced to 0,1 g/L. It was observed that zeta potential of all of the examined suspensions was positive (Fig. 1). For TiO_2 suspension zeta potential increased with pH in the range between 3.1-5.9 pH. At the higher pH the zeta drastically decreases and suspension losses its stability. At pH close to neutral the suspension starts to agglomerate after few minutes without stirring and dispersed phase falls to the bottom of the beaker. In case of chitosan, the suspension is stable in range of pH from 3.0 to 4.0, where the zeta potential takes

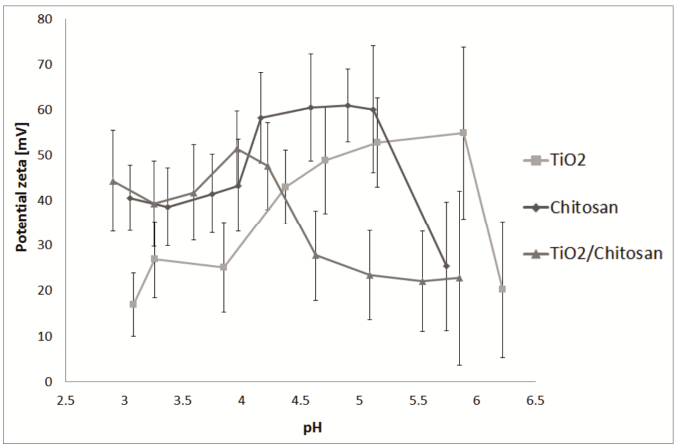

Fig. 1. The changes of zeta potential versus pH of TiO_2, chitosan and TiO_2/chitosan ethanol-water suspensions. The standard deviation error bars are depicted

values between 38.6 ±8.6-43.3 ±10.2 mV. At pH higher than 4 the zeta potential increases, it is stable between 4.2-5.1 and takes values from 58.3 ±10.0 to 60.5 ±11.8 mV. Measurement of zeta potential for TiO_2/chitosan suspensions shows two stable regions. First occurred in pH range 2.9-4.2, in which zeta potential takes values between 39.3 ±9.5-51.4 ±8.4 mV and second in pH range 4.6-5.8, where potential is lower and takes values between 22.1 ±11.0-27.8 ±9.9 mV. Under this pH value two maxima on the plot were noticed, which implied precipitation of the chitosan. Chitosan dissolves in ethanol-water solvent and its solubility increases with addition of acids [20,23]. Close to the neutral pH the stability of the chitosan solution decreases, what is associated with the decrease of its solubility. Based on the obtained results it was determined, that the optimum pH for chitosan and TiO_2 suspension is between 3 and 4.2.

Suspensions containing 0.5 g/L of chitosan and from 0.5 to 3 g/L of TiO_2 were tested and prepared for deposition of trial coatings at the constant voltage from the range between 5 and 50 V. The macroscopic images of the coatings deposited from suspensions consisted of 2 g/L TiO_2 and 0.5 g/L chitosan are shown in Fig. 2. Coatings deposited at the voltage between 14 and 16 V were characterized by the best quality. For the voltage higher than 20 V the gas bubbles, which appear as the result of water electrolysis during EPD in these conditions, destroy the surface of the coating. For the voltage between 30 and 50 V chitosan is probably degraded [24] and surfaces were covered by porous, inhomogeneous coating. Process of deposition under voltage 10 V provides a thin, non-uniform coating. The voltage parameters of the EPD process were selected to provide low bubbling gas in water electrolysis. Too intensive water electrolysis process can reduce the homogeneity of the coatings and its adhesion to the steel [25]. The time of deposition was determined in the range between 180 and 240 s. This parameter was optimized through the macroscopic observation of the coatings and analysis of the current density – time curve. At the first stage of EPD process, the current density quickly increases and reaches a constant value. When the nonconductive TiO_2/chitosan coating is deposited on most of metal surface, current was decreasing.

4. Microstructure

TEM investigation of TiO_2 powder nanoparticles used for EPD of the coatings revealed that they are oval or polygonal in shape (Fig. 3a). Their equivalent circle diameter is in the range from 14 to 85 nm. Selected area electron diffraction analysis has shown that the TiO_2 particles are the mixture of anatase (tetragonal, space group I $4_1/a$ m d) and rutile (tetragonal, primitive, space group P $4_2/m$ n m).

Top surfaces of the coatings were examined by SEM. The coatings were free of cracks and pores (Fig. 4). The imperfections in the form of agglomerations of TiO_2 nanoparticles were present. Such agglomerates have been probably not dispersed in the suspensions by the ultrasonication and thus remained in the deposited coatings. Analysis of SEM images has shown that the coatings deposited from suspensions containing higher concentration of TiO_2 nanoparticles exhibited more dense distribution of them in chitosan matrix. Figure 4a shows the uniformly deposited ceramic agglomerates in the coating deposited from suspension containing 0.5 g/L of TiO_2 the particles. For concentrations of TiO_2 from 1 to 2 g/L (Fig. 4b,c) the surface of the coatings was fully covered by those particles, but there were visible agglomerates. Coatings deposited from 3 g/L TiO_2 suspensions were fully uniform and individual particles weren't visible (Fig. 4d).

Fig. 2. EPD composite nc-TiO_2/chitosan coatings electrophoretically deposited from water/ethanol suspension with 2g/L TiO_2 and 0.5 g/L chitosan using a voltage of a) 10 V, b) 20 V, c) 30 V, d) 40 V, e) 50 V and deposition time 240 s

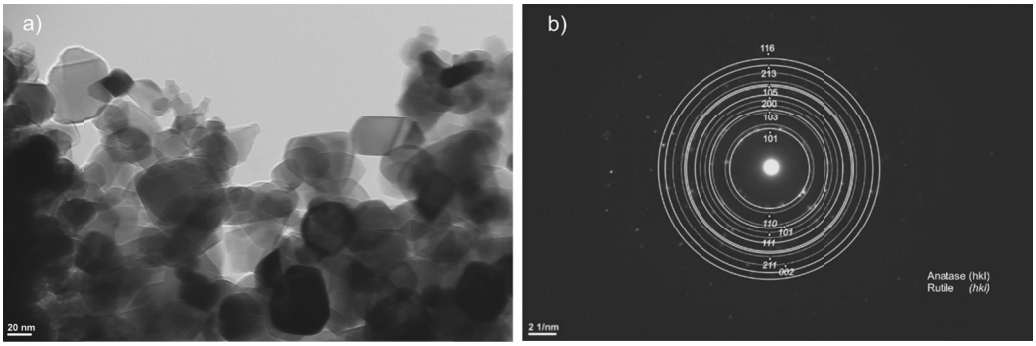

Fig. 3. a) TEM bright-field image of the TiO_2 nanoparticles used for deposition of the coatings and b) selected area electron diffraction pattern with its solution for anatase (hkl) and rutile *(hkl)*

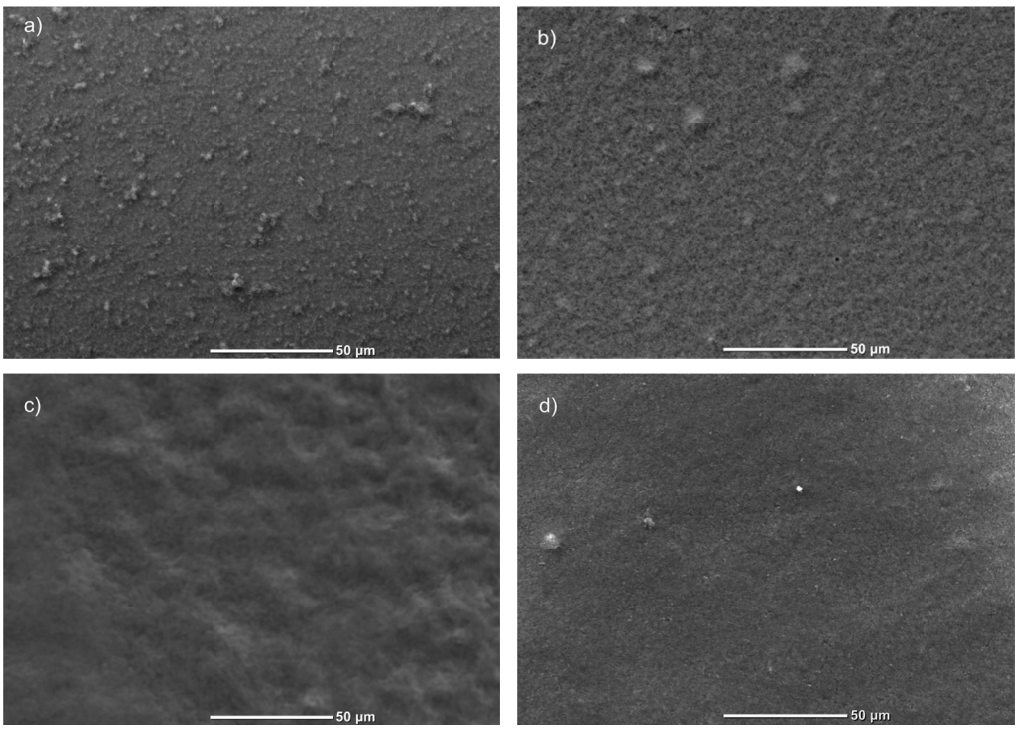

Fig. 4. SEM micrographs of coatings produced by EPD on X2CrNiMo17-12-2 steel from suspensions containing 0.5 g/L of chitosan and TiO_2 contents of: a) 0.5 g/L b) 1 g/L, c) 2 g/L, d) 3 g/L

TEM microstructural investigation was performed on the cross-section specimen prepared from the coating deposited using suspension of 3g/L TiO_2 and 0.5 g/L chitosan. Figure 5 shows the microstructure of the coating observed in TEM bright-field mode. The thickness of the coating measured on the TEM image of the cross section was 4.1 ±0.1 µm. The microstructure of the coating consisted of TiO_2 nanoparticles uniformly distributed in chitosan matrix. The coating was well bonded with the substrate. No discontinuities between the coating and the steel substrate were found.

Results of microstructural investigation of the coatings were correlated with their roughness parameters. The results of the measurements performed using the optical profilometer are given in Table 1. The smoothest surfaces were obtained for the coatings produced from suspensions containing 0.5 g/L and 3 g/L. The thickness of the coatings, measured by profile difference between the coating and exposed material substrate, was in the range 4-8 µm.

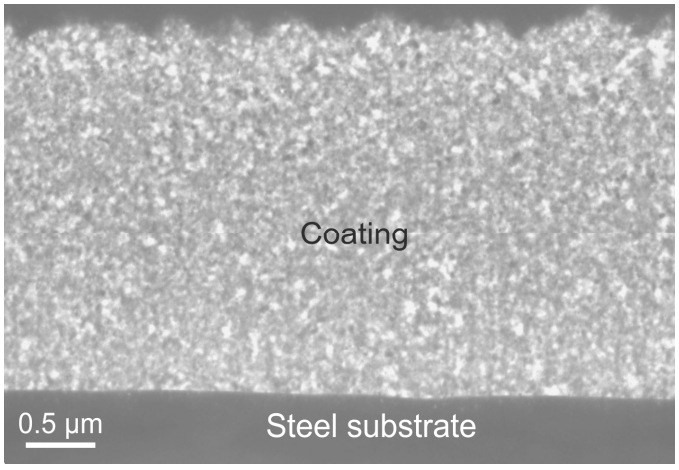

Fig. 5. TEM bright-field image of the cross section of the nc-TiO_2/chitosan coating on X2CrNiMo17-12-2 steel obtained from suspension containing 3 g/L TiO_2 and 0.5 g/L chitosan

TABLE 1

Roughness parameters of the nc-TiO_2/chitosan coatings deposited from suspensions containing form 0.5 g/L to 3 g/L TiO_2

Parameter [µm]	Coating deposited from suspension containing			
	0.5 g/L TiO_2	1.0 g/L TiO_2	2.0 g/L TiO_2	3.0 g/L TiO_2
R_a, arithmetical mean deviation of the roughness profile	0.1	0.8	0.4	0.3
R_q, root mean squared	0.2	1.1	0.6	0.4
R_z, average distance between the highest peak and lowest valley	4.9	10.6	9.3	7.4
R_t, maximum height of the roughness profile	10.8	15.8	12.8	9.9

Corrosion resistance of the materials was measured by polarization curves in Ringer's solution. This corrosive medium contained chlorides, for which the stainless steel is not resistant. The Ringer's solution in that case simulated body fluids. In this test the specimens of uncoated X2CrNiMo17-12-2 steel as well as coated by nc-TiO_2/chitosan composite coatings were used. The results are shown in Table 2 and Fig. 6. All curves for coated steel revealed higher corrosion potential E_{corr} than bare metal. For the majority of coatings (except this one deposited from the solution containing 0.5 g/L TiO_2) the values of corrosion current density

i_{corr} were lower than for bare metal. The composite coatings from suspensions containing 1-3 g/L TiO_2 were characterized by the best corrosion resistance. Not much lower values of i_{corr} than for bare steel were obtained for composite coatings deposited from suspension containing 0.5 g/L of TiO_2.

The increase of corrosion resistance may be a result of a few mechanisms. Mainly, the surface of the steel is coated and area between metal and Ringer's solution is significantly reduced. Additionally, TiO_2 particles, like most of oxides, cause a decrease of corrosion potential of the system, and therefore the increase of TiO_2 particles' concentration in the coating causes its higher corrosion resistance. Furthermore, nanoparticles of TiO_2 are small and thus oxide particles could cover coated places present in the chitosan coating [27]. Chitosan might degrade in the electrochemical process and products of its degradation can change the local pH and thus affect the electrochemical corrosion process [19,24]. Based on SEM microstructural analysis it can be concluded that the coatings with more uniform and dense distribution of TiO_2 in chitosan were characterized by better electrochemical properties.

The adhesion of the coatings to the steel substrate was studied by scratch testing. The deformation of the substrate and coatings during the test led to the shear stress concentration in the coating-substrate interface. When this stress exceeded the interface strength, the adhesion cracks were formed and coatings were removed from the surface. The critical load L_c values were determined as the applied loads at which the adhesion cracks occurred. Images of scratch tracks and cracks in the tested coatings, with L_c values indicated, are shown in Fig. 7.

TABLE 2

Corrosion potential E_{corr} measured for coated and uncoated steel in Ringer's solution

Material	Uncoated X2CrNiMo17-12-2 steel	nc-TiO_2/chitosan on X2CrNiMo17-12-2 steel from suspension containing TiO_2:			
		0.5 g/L	1 g/L	2 g/L	3 g/L
E_{corr} [V]	–0.291	–0.165	–0.110	–0.125	–0.114

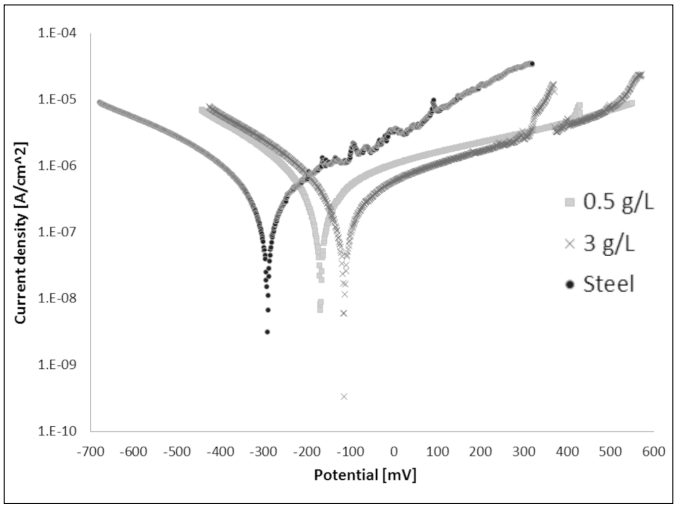

Fig. 6. Polarization curves obtained in Ringer's solution for the a) uncoated steel and nc-TiO_2/chitosan coatings produced from suspensions containing b) 0.5 g/L TiO_2, c) 1 g/L TiO_2, d) 2 g/L TiO_2, e) 3 g/L TiO_2

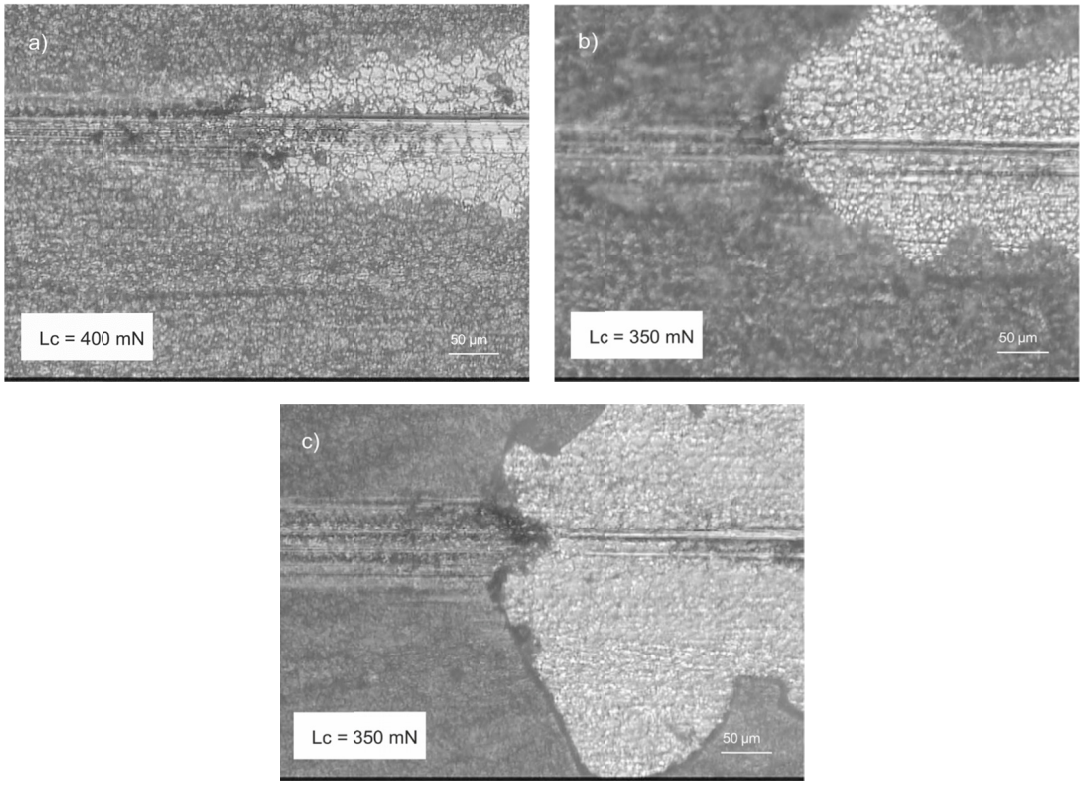

Fig. 7. LM images of scratch tracks in the coatings obtained from the suspensions containing 0.5 g/L chitosan and a) 1 g/L TiO_2, b) 2 g/L TiO_2, c) 3 g/L TiO_2

For all the tested coatings the critical load values were in the range from 350 to 400 mN. The area of delaminations grown with the increasing amount of TiO_2 in the coating. The cracks propagated far beyond the scratch tracks, especially for coatings deposited from suspension containing 2 g/L and 3 g/L of TiO_2 (Figs. 7b,c), what confirms its rather poor adhesion to the substrate. It could be a result of higher stiffness of coatings with higher ceramic phase/polymer ratio. The decrease of the adhesion to the stainless steel substrate of the polymer (alginate)/TiO_2 coatings associated with the increase of the ceramic phase fraction was observed also by Cordero-Arias and others [28]. They have postulated that the higher oxide/polymer ratio in those coatings influences the decrease of the polymer binding effect thus results in the intensification of brittle cracks in scratch tests.

5. Conclusions

In this study nc-TiO_2/chitosan composite coatings were successfully deposited on X2CrNiMo17-12-2 stainless steel substrate by EPD process. From obtained results the following conclusions can be drawn:

1. For cathodophoretic deposition of nc-TiO_2/chitosan composite coatings on X2CrNiMo17-12-2 from water-ethanol suspension (ratio 50:50) with 1% acetic acid, the optimal deposition voltage was in the range between 14 and 16 V.
2. Stability and zeta potential of the nc-TiO_2/chitosan suspension was higher in the acidic pH. The electrophoretic deposition was optimal when the suspension pH was in the range between 3.0 and 4.2.
3. The microstructure of coatings was uniform and crack-free. The lowest roughness of coatings was found for those deposited from suspension containing 0.5 g/l and 3 g/l TiO_2.
4. All deposited coatings exhibited better corrosion resistance in Ringer's solution that the uncoated X2CrNiMo17-12-2 steel.
5. The scratch tests have showed that the adhesion of the nc-TiO_2/chitosan coatings to the stainless steel substrate was rather poor and depended on the polymer/ceramic phase ratio in the coating.

Acknowledgments

The work was supported by the statutory project of AGH-UST no. 11.11.110.293.

The authors kindly acknowledge the company JEOL (EUROPE) SA branch in Poland for allowing access to the JEOL scanning electron microscope JCM-6000 NeoScope II for this investigation. We also would like to thank Marta Gajewska, PhD for the preparation of the FIB lamella at ACMiN AGH. The valuable contribution in experiments of Izabela Kalemba – Rec, PhD, as well as Tomasz Ratajski, MSc and D. Jugowiec, MSc, all from AGH-UST, is gratefully acknowledged.

REFERENCES

[1] J.A. Disegi, L. Eschbach, Injury **31**, D2 (2000).
[2] J. Walczak, F. Shahgaldi, F. Heatley, Biomaterials **19**, 229 (1998).
[3] Chun-Che Shih, Chun-Ming Shih, Yea-Yang Su , Lin Hui Julie Su, Mau-Song Chang, Shing-Jong Lin, Corros. Sci. **46**, 427 (2004).
[4] G. Bordji, J.-Y. Jouzeau, D. Mainard, E. Payan, J.-P. Delagoutte, P. Netter, Biomaterials **17**, 491 (1996).
[5] J.H. Park, J.S. Kim, J.M. Park. Surf. Coat. Tech. **8**, 172 (2013).
[6] L. Visai, L. De Nardo, C. Punta, L. Melone, A. Cigada, M. Imbriani, C.R. Arciola, Int. J. Artif. Organs. **34** (9), 929 (2011).
[7] H. Haick, Y. Paz, J. Phys. Chem. B **105** (15), 3045 (2001).
[8] L.C Gerhardt, G.M.R. Jell, A.R. Boccaccini, J. Mater. Sci.: Mater. Med. **18**, 1287 (2007).
[9] K.A.M. Amin, M. Panhuis, Polymers **4**, 590 (2012).
[10] Fei Chen, Zhou-Cheng Wang, Chang-Jian Lin, Mater. Lett. **57**, 858 (2002).
[11] H. Honarkar, M. Barikani, Monatsh. Chem. **140**, 1403 (2009).
[12] L.L. Shaw, D. Goberman, R. Ren, M. Gell, S. Jiang, Y. Wang, T.D. Xiao, P.R. Strutt, Surf. Coat. Tech. **130**, 1 (2000).
[13] A. Góral, L. Lityńska-Dobrzyńska, W. Zórawski, K. Berent, J. Wojewoda-Budka, Arch. Metall. Mater. **58**, 335 (2013).
[14] D. Velten, V. Biehl, F. Aubertin, B. Valeske, W. Possart, J. Breme, J. Biomed. Mater. Res. A. **59**, 18 (2002).
[15] D.P. Macwan, Pragnesh N. Dave, Shalini Chaturvedi, J. Mater. Sci. **46**, 3669 (2011).
[16] X. Nie, A. Leyland, A. Matthews, Surf. Coat. Tech. **125**, 407 (2000).
[17] Y. Han, D.H. Chen, L. Zhang, Nanotechnology **19**, 335 (2008).
[18] D. Hanaor, M. Michelazzi, P. Veronesi, C. Leonelli, M. Romagnoli, C. Sorrell, J. Eur. Ceram. Soc. **31**, 1041 (2011).
[19] L. Cordero-Arias, S. Cabanas-Polo, H. Gao, J. Gilabert, E. Sanchez, J.A. Roether, D.W. Schubert, S. Virtanen, A.R. Boccaccini, RSC Advances **3**, 11247 (2013).
[20] N.S. Raddaha, L. Cordero-Arias, S. Cabanas-Polo, S. Virtanen, J.A. Roether, A.R. Boccaccini, Materials **7**, 1814 (2014).
[21] T. Moskalewicz, A. Czyrska-Filemonowicz, A.R. Boccaccini, Surf. Coat. Tech. **201**, 7467 (2007).
[22] Laxmidhar Besra, Meilin Liu, Progress in Materials Science **52**, 1 (2007).
[23] H.Z. Abdullah, C.C. Sorrell, J. Aust. Ceram. Soc. **44** (2), 12 (2008).
[24] I. Zhitomirsky, A. Hashambhoy, J. Mater. Process. Tech. **191**, 68 (2007).
[25] Q. Cai, Z. Gu, Y. Chen, W. Han, T. Fu, H. Song, F. Li, Carbohyd. Polym. **79**, 783 (2010).
[26] L. Besra, T. Uchikoshi, T.S. Suzuki, Y. Sakka, J. Eur. Ceram. Soc. **30**, 1187 (2010).
[27] G. Grundmeier, W. Schmidt, M. Stratmann, Electrochim. Acta **45**, 2515 (2000).
[28] L. Cordero-Arias, S. Cabanas-Polo, J. Gilabert, O.M. Goudouri, E. Sanchez, S. Virtanen, A.R. Boccaccini, Adv. Appl. Ceram. **113**, 42 (2014).